This is the post-print version of the manuscript published in

Inorganic Chemistry, 2018, vol. 57, p. 3411-3419, ISSN: 0020-1669, doi: 10.1021/acs.inorgchem.8b00177

Insight into the Electrochemical Reduction Mechanism of Pt(IV) Anticancer Complexes.

*Iogann Tolbatov, Cecilia Coletti, Alessandro Marrone and Nazzareno Re**

Dipartimento di Farmacia, Università degli Studi "G. D'Annunzio" Chieti-Pescara, Via dei Vestini, I-66100 Chieti, Italy

AUTHOR EMAIL ADDRESS nre@unich.it

ABSTRACT

We carried out a theoretical study on the mechanism of electrochemical reduction of the prototypical platinum(IV) anticancer complex $[Pt(NH_3)_2(CH_3COO)_2Cl_2]$ to the corresponding platinum(II) $[Pt(NH_3)_2Cl_2]$ derivative.

Energies and geometric structures of the original Pt(IV) complex and all possible Pt(III) and Pt(II) intermediates and transition states involved in the reduction process have been calculated using density functional theory and Møller–Plesset perturbation theory. This study allowed us to formulate a detailed mechanism for the two-electron reduction of the $[Pt^{IV}(NH_3)_2(CH_3COO)_2Cl_2]$ complex.

The results show that, in agreement with the experimental evidence from cyclic voltammetry, the initial one electron reduction of the $[Pt^{IV}(NH_3)_2(CH_3COO)_2Cl_2]$ complex occurs through a stepwise mechanism via a metastable hexacoordinated platinum(III) $[Pt^{III}(NH_3)_2(CH_3COO)_2Cl_2]-$ intermediate and a subsequent acetate ligand detachment with an activation free energy of 5.1 kcal mol^{-1}. On the other hand, the second electron reduction of the resulting pentacoordinated $[Pt^{III}(NH_3)_2(CH_3COO)Cl_2]$ species occurs through a barrierless concerted process to the final $[Pt^{II}(NH_3)_2Cl_2]$ derivative.

KEYWORDS

1. Introduction.

Cisplatin, cis-diamminedichloro-platinum(II) or $[(NH_3)_2PtCl_2]$, is one of the most widely used antitumor drugs and is most active against a variety of tumors, especially testicular and ovarian cancers.[1-9] However, its clinical success is limited by severe side effects which have led to the development of new platinum compounds with improved pharmacological properties such as the

second-generation Pt-based anticancer drug carboplatin, cis-diammine(cyclo-butane-1,1-dicarboxylato)-platinum(II), or the third-generation drug oxaliplatin, (1R,2R-diaminocyclohexane)oxalato-platinum(II),[10-12] which have already entered clinical use. Another promising approach to overcome the drawbacks of Pt(II) drugs is to utilize six-coordinate Pt(IV) complexes that can act as pro-drugs undergoing reduction once inside the target cell (by biological reducing agents such as ascorbate or glutathione) to afford the active, four-coordinate, square planar Pt(II) analogues before binding to their ultimate target DNA.[13-16] The relative inertness of low spin d^6 Pt(IV) complexes prevents from most side effects of Pt(II) complexes, especially those related to early hydrolysis and binding to plasma proteins, and allows oral administration of the drug. The reduction from Pt(IV) to Pt(II) is accompanied by the loss of two axial ligands and has been extensively investigated by both chemical and electrochemical approaches.[17] In particular, electrochemical studies, mainly by cyclic voltammetry, have been thoroughly employed to explore the redox behavior of Pt(IV) antitumor complexes and all of them exhibit a single irreversible reduction event. Therefore, these studies provide only a peak potential for the irreversible reduction rather than the standard redox potential for the Pt(IV)/Pt(II) couple. Moreover, the occurrence of a single and irreversible two-electron wave in the voltammograms indicates that electrochemical and chemical steps involved in the reduction process are strongly coupled within the technique time scale and makes it difficult the use of standard voltammometric approach to characterize the mechanism of the Pt(IV) to Pt(II) reduction. Although the peak potentials from cyclic voltammetry have often been employed as a measure of the ease of reduction of the corresponding complexes, they do not always correlate with the rates of reduction by biological reducing agents, which depend not only on the rate of the electron transfer to the metal center but also on the energy barrier for the loss of the two axial ligands. It is therefore not surprising that, in spite of several studies, there is no direct correlation between peak potentials and *in vitro* or, even less, *in vivo* cytotoxic activity. However, a detailed knowledge of the mechanism of Pt(IV) reduction would be of great value in understanding the dependence of the rate of reduction on the nature of the axial ligands and possibly correlating it with simple electrochemical parameters such as the reduction potential of the complexes, opening the way for a rational design of more active Pt(IV) antitumor drugs.[18]

In a recent study,[19] a series of electrochemical experiments have been employed to study the mechanism for the two-electron reduction of $Pt^{IV}(NH_3)_2Cl_2L_2$ to $Pt^{II}(NH_3)_2Cl_2$ (L = CH_3COO^-, $CHCl_2COO^-$ and Cl^-) and have allowed to show that electron transfer and Pt−L bond cleavage occur in a stepwise fashion, thus suggesting the formation of a metastable six-coordinate Pt(III) intermediate upon the first electron addition, while the loss of both axial ligands occurs with the second electron transfer, and to extract the standard reduction potential E_1^0 for the Pt(IV)/Pt(III) couple from the irreversible peak potential in the cyclic voltammogram within the framework of

Marcus theory. In the same study, density functional calculations were carried out on thermodynamics of the two electron reduction process, allowing a reliable estimate for the standard reduction potential E_1^0, but no detailed calculation was carried out on the mechanism of reduction of $Pt^{IV}(NH_3)_2Cl_2L_2$.

In this paper we carried out a theoretical study on the thermodynamics and the kinetics of the expected key steps in the mechanism of electrochemical reduction of the same platinum(IV) $[Pt(NH_3)_2(CH_3COO)_2Cl_2]$ complex to the corresponding platinum(II) $[Pt(NH_3)_2Cl_2]$ derivative, i.e. cisplatin, aiming at characterizing all possible Pt(III) and Pt(II) intermediates and transition states during the reduction process and to formulate a detailed mechanism for the two-electron reduction of the $[Pt^{IV}(NH_3)_2(CH_3COO)_2Cl_2]$ complex.

Indeed, a deeper insight into the dependence of the mechanism of reduction of Pt(IV) complexes would be very important to understand its mechanism of action *in vivo* and may be useful to design new and more potent platinum(IV) anticancer drugs.

2. Computational Details.

All calculations were performed with the Jaguar 9.1[20,21] and Gaussian09[22] quantum chemistry packages.

Optimizations were carried out in gas phase using the density functional theory (DFT) with the B3LYP hybrid functional,[23,24] which is known to give a good description of geometries and reaction profiles for transition metal-containing compounds[25,26] including platinum(II)[27-32] and a few platinum(IV)[33,34] based anticancer compounds. Other latest-generation functionals explicitly developed for systems with long-range electron correlations were used for benchmarking such as M06,[35] M06-2X,[35] as well as the dispersion-corrected M06-D3[35] and long-range-corrected version of B3LYP using the Coulomb-attenuating method CAM-B3LYP-D3[36] with Grimme's dispersion correction.[37] The Møller-Plesset perturbative approach MP2[38-40] was used as well to obtain a more explicit picture of the process. Indeed, in a recent study,[41] it was used quite successfully for computation of the structural parameters and vibrational frequencies of platinum(II) anticancer complexes.

All geometrical optimizations have been carried out with the LACV3P**++ basis set.[42] This basis set describes the 1s-4d core electrons of the platinum atom with the Hay and Wadt core-valence relativistic (i.e. with an implicit treatment of scalar-relativistic effects) effective core-potential (ECP) leaving the outer 18 electrons of platinum as well as electrons of the remaining atoms to be treated explicitly by the 6-311++G** basis set of triple-ζ quality. Single point electronic energy calculations were performed on the gas-phase geometries with the augmented correlation consistent basis sets

aug-cc-pVDZ and aug-cc-pVTZ (in this case the corresponding aug-cc-pVTZ pseudo potential was employed for the platinum atom).[43-45]

Frequency calculations were performed to verify the correct nature of the stationary points and to estimate zero-point energy (ZPE) and thermal corrections to thermodynamic properties. Intrinsic reaction coordinate (IRC) calculations were employed to locate reagents and products minima connected with the transition states for each considered reaction step.

The Poisson-Boltzmann (PB) continuum solvent method was used to describe the solvation and represents the solvent as a layer of charges at the molecular surface, serving as a dielectric continuum boundary, thus accounting for detailed molecular shape.[46] Solvation energies were calculated on gas-phase stationary points with the same basis set employed for single point calculations, except for MP2 results where the solvation energies were those calculated at the B3LYP/LACV3P**++ level of theory, taking a dielectric constant of 80.37 for water and the standard set of optimized radii in Jaguar. CPCM solvent model was also employed and found to give results similar to PB method (an example is reported in Table S1 in Supporting Information).

Enthalpies and Gibbs free energies were obtained at 298.15 K and 1 atm from total electronic energies including ZPE, thermal and entropic corrections, following standard statistical procedures, and adding solvent corrections. ZPE, thermal and entropic corrections were always obtained at the considered level of theory, except for MP2 results, where the values calculated at the B3LYP/LACV3P**++ level of theory were employed.

3. Results and Discussion.

A full comprehension of the reductive activation of the Pt(IV) complex into its Pt(II) derivative requires a detailed identification of all intermediates and transition states of the overall reaction and understanding how they are coupled to one another. The electrochemical potential for the reductive activation of the prodrug is determined by the energy involved in the addition of two electrons to the Pt(IV) center and the energetics associated to the loss of two ligands. The experimentally observable redox properties are therefore the result of a complex entangling of electrochemical and chemical events and are thus strictly connected to the detailed mechanism of the Pt(IV) prodrug activation reaction.

The reduction of $[Pt^{IV}(NH_3)_2(CH_3COO)_2Cl_2]$ to $[Pt^{II}(NH_3)_2Cl_2]$ occurs through the addition of two electrons and the loss of the two axial ligands: in order to consider all possible elementary steps, the process has been decomposed in uncoupled single electron addition and ligand loss steps as reported in Figure 1 where vertical arrows (lightning bolt arrows) correspond to one electron addition without any ligand loss, while horizontal lines correspond to the loss of an axial ligand without electron addition. DFT calculations were therefore carried out on the thermodynamics and the kinetics of all

the steps and allowed to calculate the reduction potential for every one-electron reduction step and the reaction and activation free energy for every ligand loss process thus shedding light onto the detailed mechanism for the two-electron reduction of the $[Pt^{IV}(NH_3)_2(CH_3COO)_2Cl_2]$ complex. Several DFT exchange-correlation functionals have been used as well as the high-level ab initio Møller-Plesset perturbation theory for the analysis of reaction path, in order to increase the reliability and possibly the accuracy of the results. In the following we will consider the B3LYP values and report the results obtained with other DFT functionals and the MP2 approach only for a more thorough discussion of the key steps.

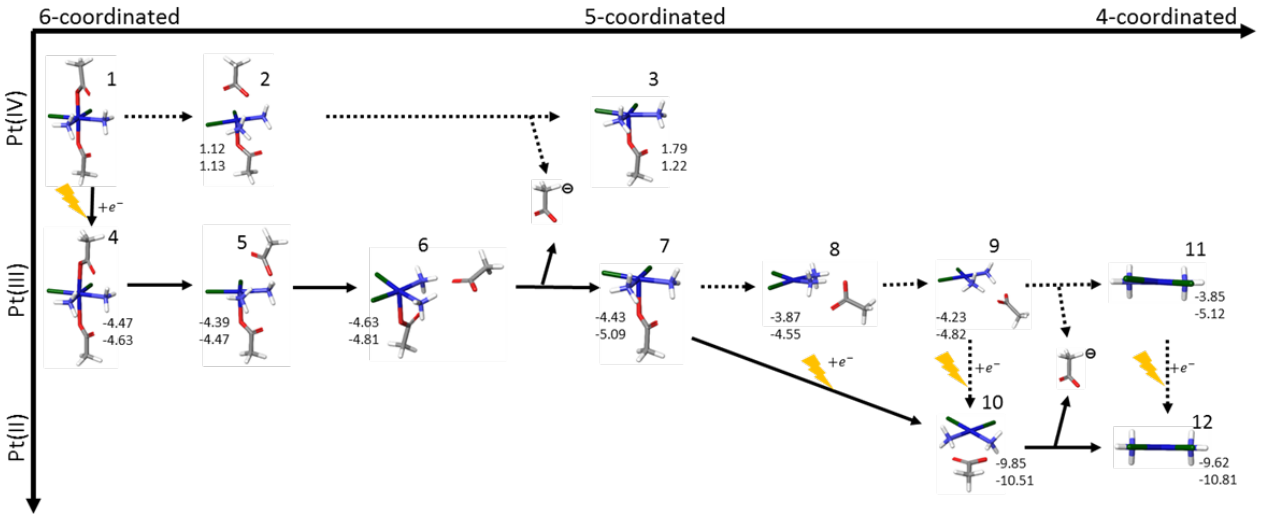

Figure 1. Two-electron reduction of the six-coordinated Pt(IV) complex. The geometries are obtained as the most stable structures in gas phase, whereas enthalpy (upper) and free energy (lower) values, in eV, are calculated in the solution phase.

Each of the considered ligand loss steps was investigated by taking into account that the leaving ligand can form stable non-covalent adducts prior full departure as for Pt(II) complexes.[47-49] For each step, we have thus optimized the geometries of the reactant (R), transition states (TS), product adducts (PA) and final products. The corresponding activation and reaction enthalpies and free energies have been calculated relatively to the reactants and to the lowest between the product adducts or products infinitely apart, respectively.

The geometries of the most stable structures are reported in Figure 1 where the activation and reaction enthalpies and free energies at the B3LYP level are summarized for the main steps. The complete energetics of the processes, including all the structures which have been considered in the calculations, is available in Figure S1 in the Supporting Information. The free energy values calculated for the most stable species are reported at Table 1, while all the examined species at all the considered levels of theory are reported in Table S2, and the free energy profile of the overall

reaction is depicted in Figure 2. The corresponding enthalpy values are reported in Tables S3 – S5 and Figure S2.

Table 1. Relative Gibbs free energies at 298 K in solution for the species involved in the reaction profile of Fig.2. All values in eV. Last row (bold face): Calculated redox potentials for the Pt(IV) complex **1**, in Volt.

Structures	PB/B3LYP/LACV3P**++	PB/B3LYP/aug-cc-pVTZ	PB/CAM-B3LYP-D3/LACV3P**++	PB/M06/LACV3P**++	PB/M06-D3/LACV3P**++	PB/M06-2X/LACV3P**++	PB/M06-2X/aug-cc-pVTZ	PB/MP2/aug-cc-pVDZ	PB/MP2/aug-cc-pVTZ
1	0.00	0.00	0.00	0.00	0.00	0.00	0.00	0.00	0.00
4	-4.63	-4.35	-4.69	-4.76	-4.76	-4.97	-4.61	-3.58	-3.61
5	-4.47	-4.22	-4.44	-4.50	-4.49	-4.70	-4.37	-3.35	-3.39
6'	-4.77	-4.48	-4.65	-4.64	-4.62	-4.49	-4.45	-3.47	-3.53
6	-4.81	-4.52	-4.69	-4.66	-4.64	-4.88	-4.48	-3.50	-3.57
7	-5.09	-4.79	-4.82	-4.90	-4.84	-5.11	-4.59	-3.67	-3.77
7'	-5.01	-4.79	-4.70	-4.78	-4.72	-4.96	-4.59	-3.52	-3.63
7''	-4.69	-4.48	-4.42	-4.55	-4.49	-4.72	-4.37	-3.24	-3.34
8	-4.55	-4.45	-4.29	-4.00	-3.93	-3.69	-4.04	-2.66	-2.77
8'	-4.44	-4.25	-4.13	-4.11	-4.05	-4.46	-3.80	-2.44	-2.58
9'	-4.83	-3.90	-2.34	-4.65	-4.59	-2.80	-3.61	-2.36	-3.35
9	-4.82	-4.91	-4.53	-4.14	-4.09	-3.81	-4.39	-3.03	-3.25
10	-10.51	-10.21	-10.18	-10.37	-10.31	-10.58	-10.13	-9.06	-9.30
11	-5.12	-5.10	-4.61	-4.56	-4.46	-3.92	-4.57	-3.42	-3.28
12	-10.81	-10.60	-10.28	-10.58	-10.48	-10.77	-10.39	-9.22	-9.51
$\boldsymbol{E^0_{rel}}$	**0.20**	**-0.08**	**0.26**	**0.33**	**0.33**	**0.54**	**0.18**	**-0.85**	**-0.83**

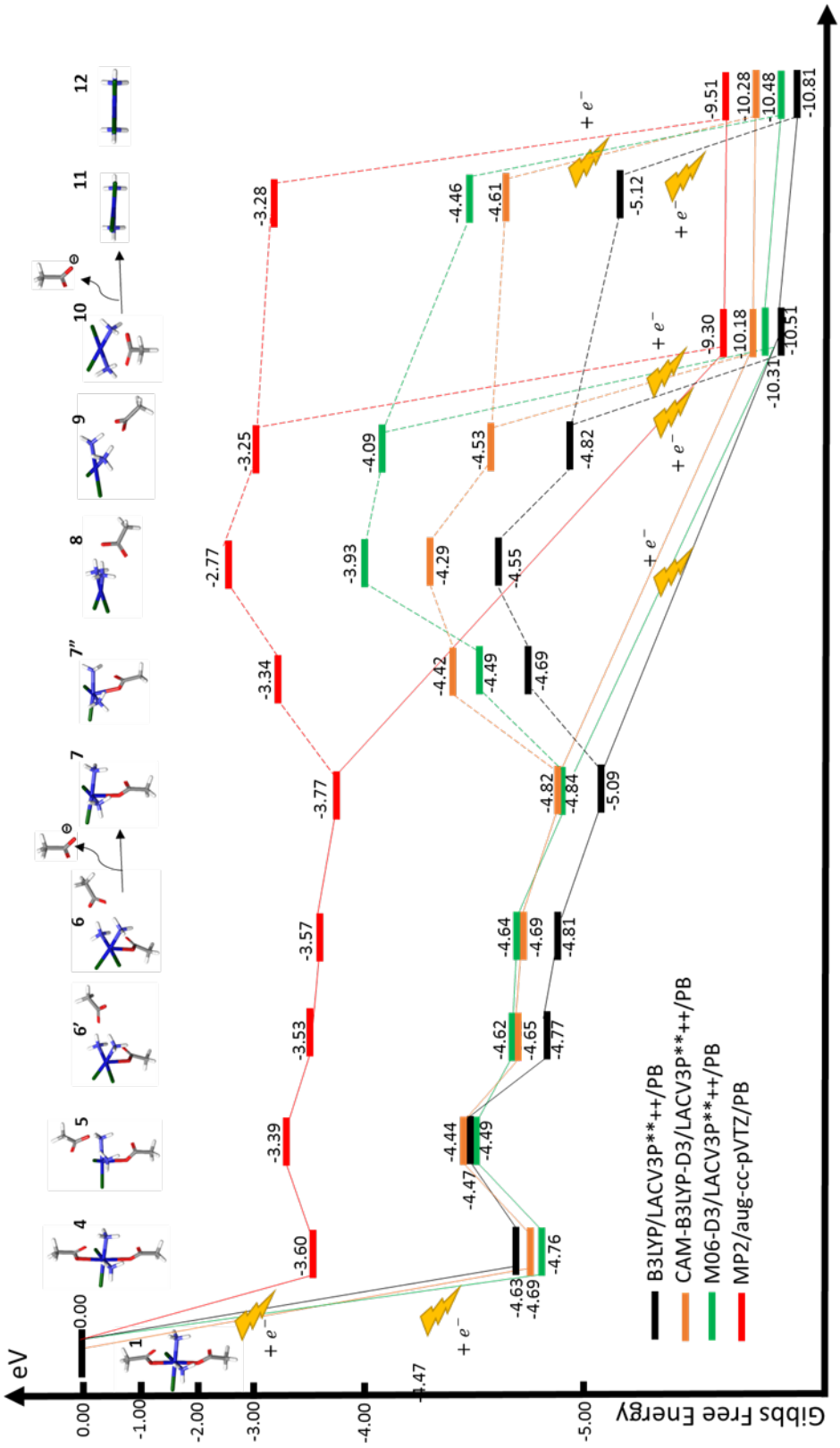

Figure 2. Gibbs free energies in solution for the reaction profile. All values in eV. The addition of one electron is denoted by a lightning.

We preliminarily considered the ligand loss from the neutral platinum(IV) anticancer complex $[Pt^{IV}(NH_3)_2Cl_2(CH_3COO)_2Cl_2]$, **1**, and a high activation free energy was found for the breaking of

the covalent bond between the acetate ligand and the Pt(IV) center, 1.13 eV, with the subsequent complete detachment of ligand at the free energy of 1.22 eV. Both these values completely prevent the system going toward this direction in agreement with the well-known stability of hexacoordinated Pt(IV) complexes so that this process does not deserve further investigation. This value is consistent with that calculated for the barrier for the Pt(IV)-acetate hydrolysis in the same Pt(IV) complex, i.e. 1.10 eV according to a recent study.[34] The addition of one electron to **1** yields a substantial free energy gain of -4.63 eV and leads to a metastable hexacoordinated $[Pt^{IV}(NH_3)_2Cl_2(CH_3COO)_2Cl_2]$ species, **4**. The metastable species **4** has two closely-separated conformers **4'** and **4"**, differing only for the relative orientation of the two *trans* acetate ligands (Figure S1). The added electron populates a metal-ligand antibonding orbital so that a weakening of the metal acetate bond is expected. Moreover, an analysis of the NBO charges of the considered species (Table S6) shows that the injected electron in **4** is not localized on the Pt atom but rather on the leaving carboxylate species. On the other hand, the charges on the Pt center significantly increase only upon the full detachment of one carboxylate anion in the transition state **5** and product-adduct **6**. Indeed, when we analyzed in detail the thermodynamics and the kinetics of the acetate ligand loss from **4**, a small barrier has been found for the breaking of the platinum-acetate bond, ranging from 0.13 (B3LYP) to 0.27 eV (M06-D3) (Tables 2 and S5). A late transition state **5** was found, showing an elongated Pt-O bond (3.31 Å), evolving into product-adduct species where the leaving acetate is linked to the pentacoordinated metal centre via hydrogen bonds with the amine ligands, **6**. Two possible conformers were found, **6** and **6'**, differing for the presence of one or two hydrogen bonds, respectively. The complete detachment of the negatively charged acetate ligand, leading to a stable pentacoordinated $[Pt^{III}(NH_3)_2Cl_2(CH_3COO)]$ species, **7**, is a slightly endothermic albeit exoergonic process with a reaction enthalpy of 0.20 eV and a reaction free energy of -0.28 eV. We also investigated the detachment of the remaining acetate ligand from **7** finding a transition state, **8**, with an elongated Pt-O bond (3.50 Å) that evolves into an adduct, **9**, where the acetate is still bound to a tetracoordinated $[Pt^{III}(NH_3)_2Cl_2]^+$ species via hydrogen bonds with the amine ligands. The complete detachment of the acetate ligand, leading to the final $[Pt^{III}(NH_3)_2Cl_2]^+$ species, **11**, is a slightly exoergonic process with a free energy of -0.30 eV. A relatively high activation free energy of 0.54 eV (even higher when calculated at MP2 level or employing the Minnesota functionals) was found, so that an irreversible evolution of the Pt(III) complex **7** along this channel before the second electron reduction can be ruled out.

The addition of the second electron to **7** is accompanied by an energy decrease of 5.42 eV and is coupled with the detachment of the second acetate ligand leading directly to the hydrogen-bonded adduct of cisplatin with the acetate anion **10**. The complete detachment of the acetate anion, leading to the final cisplatin product, is an easy process with a free energy decrease of 0.3 eV. The NBO

charge analysis shows that, at variance with the first reduction step, the second electron injected in **10** is mostly localized on the Pt center and only to a lesser extent on the carboxylate leaving ligand.

These results indicate that the most stable Pt(IV), Pt(III) and Pt(II) species are those with hexa- penta- and tetra-coordinated geometries, respectively, and show an overall "potential inversion" situation whereby the Pt(III) to Pt(II) reduction is more favorable than that from Pt(IV) to Pt(III), 5.42 vs. 4.63 eV, which accounts for the instability of the Pt(III) intermediate toward disproportionation and for the occurrence of a single two electron wave in the cyclic voltammogram. The instability of Pt(III) complex toward reduction accounting for the occurrence of only one two electron wave in cyclic voltammetry is related to the high exothermicity for the cleavage of the second acetate upon electron injection, i.e. -5.62 eV, and the slight endothermicity for the detachment of the first acetate from the pentacoordinated Pt(III) complex, i.e. 0.28 eV. In addition, the identification of the transition states for the axial ligand loss steps and the evaluation of the corresponding activation energies allows to disentangle the timing of the electrochemical and chemical steps and understand the overall redox reaction.

In particular, the analysis of the first reduction step allows to address from a theoretical point of view the timing of the electron transfer and the ligand loss shedding light to its concerted or stepwise nature which has been the subject of a recent cyclic voltammetry study using the experimental protocol suggested by Savéant within the framework of the Marcus theory.[19] Indeed, the electron transfer and ligand detachment of the first reduction process, that may occur in a concerted or stepwise fashion (see Scheme 1) leading to different values of the first reduction potential E_1^o, has been shown to occur stepwise.

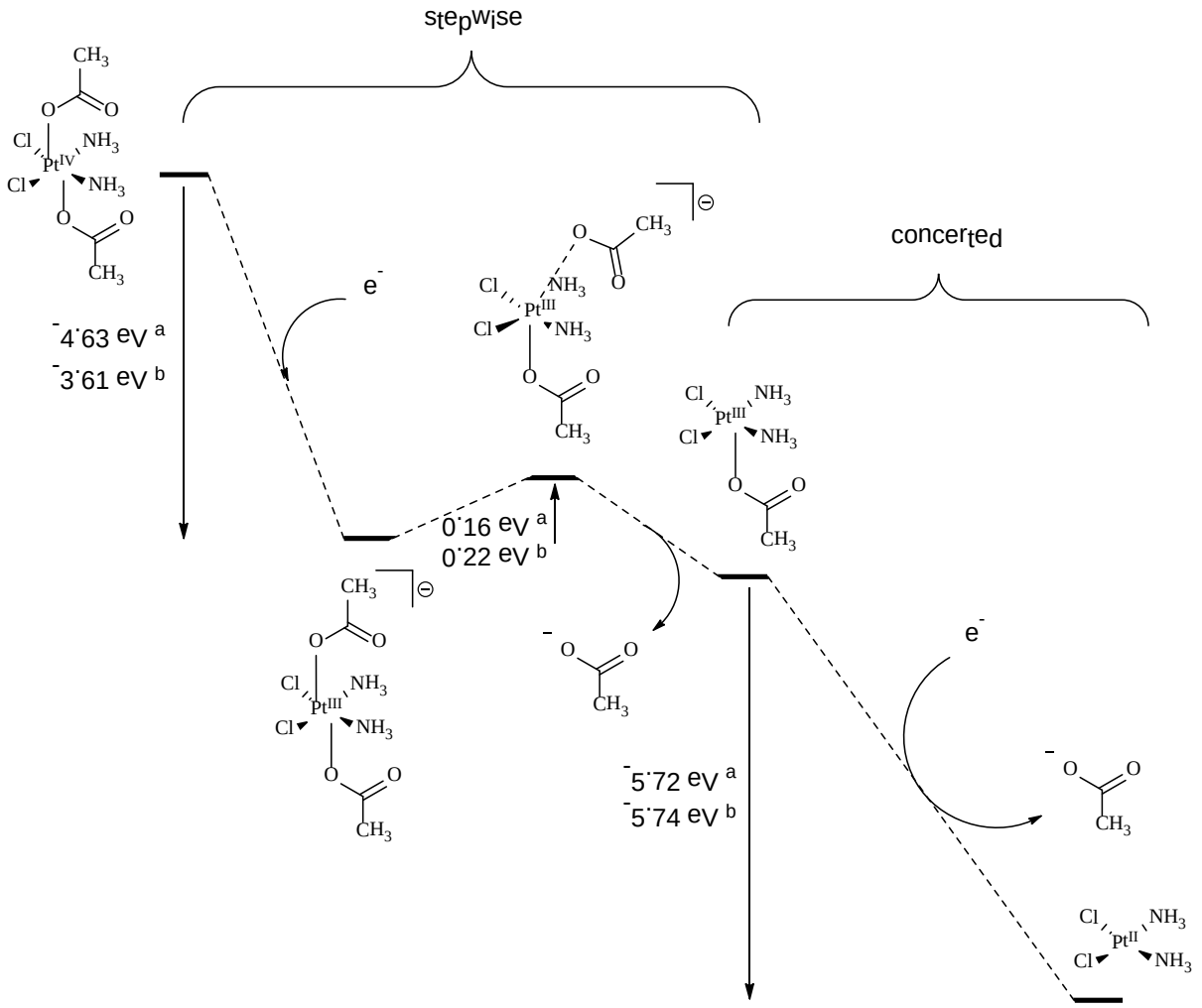

Scheme 1. Free energy profile of the two-electron reduction of **1**. [a] Values calculated at PB/B3LYP/LACV3P**++ level of theory. [b] Values calculated at PB/MP2/aug-cc-pVTZ level of theory.

Our calculations indicate that the ligand loss from the hexacoordinated platinum(III) $[Pt^{III}(NH_3)_2(CH_3COO)_2Cl_2]^-$ species initially formed upon electron transfer, although thermodynamically favorable (with a free energy gain of –0.46 eV), shows an activation barrier of 0.22 eV (MP2/aug-cc-pVTZ) toward the subsequent acetate ligand detachment (Table 2).

Table 2. Gibbs free energies in solution for the 1st ligand cleavage. All values in eV.

Method	ΔG		
	$\Delta G^{\neq}$ (4->5)	ΔG for the formation of the product adduct (4->6)	ΔG for the complete dissociation (6->7)
PB/B3LYP/LACV3P**++	0.16	-0.17	-0.28
PB/B3LYP/aug-cc-pVTZ	0.13	-0.18	-0.26
PB/CAM-B3LYP-D3/LACV3P**++	0.25	0.00	-0.13
PB/M06/LACV3P**++	0.26	0.11	-0.24
PB/M06-D3/LACV3P**++	0.27	0.12	-0.20
PB/M06-2X/LACV3P**++	0.27	0.10	-0.23
PB/M06-2X/aug-cc-pVTZ	0.23	0.13	-0.11
PB/MP2/aug-cc-pVDZ	0.23	0.07	-0.17
PB/MP2/aug-cc-pVTZ	0.22	0.04	-0.20

Such a barrier is high enough to ensure a sufficiently long life time for the hexacoordinated platinum(III) species and thus indicates a stepwise process in agreement with the experimental results. Moreover, the barrier for the ligand detachment arises from the full breaking of the covalent Pt-acetate bond rather than from a non-covalent interaction between the detached acetate anion and the Pt(III) penta-coordinate product of the reduction process.

A possible explanation to the stepwise versus synchronous occurrence of electron injection and carboxylate detachment is provided by natural bond orbital analysis on the species intercepted along the main reaction pathway, i.e. structures **1**, **4**, **5**, **6**, **7**, **10**, and **12** (Tables S6 and S7). As already discussed above, the injection of the first electron to the hexacoordinated Pt(IV) structure **1** leading to the Pt(III) structure **4** causes an overall increase of negative charge that is mainly redistributed on ligands and the subsequent detachment of carboxylate is accompanied by an increased and localized

polarization of the breaking Pt-O bond while other charge basins are almost unchanged. We have noticed that the negative charges in the leaving acetate are -0.47, -0.72, -0.91, -0.92 in structures **1**, **4**, **5**, and **6**, respectively (Table S6). This is the sign of the fact that the heterolytic breaking of the Pt-O bond is increasingly more favored. After the first electron injection, the Pt-O bond polarization is thus not sufficient for promoting a barrierless heterolysis, so that a further barrier - through transition state **5** - should be encompassed. On the other hand, the second electron injection causes a similar overall redistribution of the negative charge, although in this case the charge of detaching carboxylate is already -0.72 in structure **7**. This implies that the increased polarization of Pt-O bond upon injection of one electron is sufficient to promote a barrierless heterolysis.

Although the goal of this article was to investigate the mechanism of the electrochemical reduction of the Pt(IV) complex **1** and not the accurate estimation of its redox potentials, that is a very delicate matter deserving a separate study due to the high sensitivity to the choice of method of calculation, we did calculate the redox potential for the first electron reduction for which an experimental estimate of -0.019 V was obtained by Baik et al. through the Saveant approach.[19] The reduction potential was computed via $E_1^0 = -\Delta G_1 - 4.43\,V$, where ΔG_1 is the Gibbs free energy in solution for the one electron attachment to **1** and 4.43 V is the absolute potential of the standard hydrogen electrode in water. The relative potentials calculated by various density functionals and basis sets are shown in the last row of Table 1. A very good agreement, -0.08 V, was obtained at B3LYP/ aug-cc-pVTZ level – which was already shown to lead to accurate redox potentials[50] - but relatively large deviations were observed for other DFT functionals and even more for MP2, underlining the necessity of further benchmark studies focusing on DFT and ab initio approaches for an accurate description of the redox potentials.

4. Conclusions and further remarks

The electrochemical reduction of Pt(IV) complexes is difficult to characterize due to the irreversibility of the reduction, preventing a precise evaluation of the redox properties of the Pt(IV/II) couple. Indeed, the reduction is a two-electron redox process, which is commonly observed as a single voltammetric event, whose overall thermodynamics and kinetics is strongly influenced by the timing of the axial bond cleavage. These studies have provided some valuable insight, but the peak potential of an irreversible redox reaction is highly dependent on the scan rate and on other experimental conditions, posing serious questions about the relevance of these potentials for understanding the redox behavior of the Pt(IV) drugs. In addition, the physical meaning of the two-electron wave remains obscure when the extent of coupling between the underlying electrochemical and chemical steps within the time scale of the measurement is not known. The emerging mechanistic insight from these studies can be significantly enhanced by augmenting them with

detailed quantum chemical models. This combination allows for constructing an unprecedentedly precise model for the overall redox reaction, including a quantitative interpretation of the single two-electron response and projections for the behavior of the Pt(IV) prodrugs in biological environments.

Theoretical approaches are of invaluable help in shedding light into the details of the electrochemical reduction mechanism but they have limited to the evaluation of redox potentials of the Pt(IV/II) couple. Over the past decade, it was demonstrated that density functional theory (DFT) combined with continuum solvation models constitutes a sufficiently accurate model for evaluating the energies of even complex redox processes[51-54] with redox potentials being reproduced within ~100 mV. Typically, these calculations assume Nernstian behavior of the redox pairs and only afford standard potentials, because they do not provide any information about the kinetics of electron transfer or the existence of metastable intermediates. The strengths of this computational electrochemistry approach are that it allows for the detailed examination of the electronic structure of the redox intermediates and it is complementary to the experimental explorations. As these calculations simply locate redox intermediates, the methodology is not limited to Nernstian redox couples *per se.* It should be possible to employ the same modeling techniques to non-Nernstian behavior, provided that the kinetic information leading to deviations from standard equilibrium thermodynamics is taken from a different means, in this case from experiments. Here, we formulate a detailed mechanism for the two-electron reduction of the $[Pt^{IV}(NH_3)_2(CH_3COO)_2Cl_2]$ complex demonstrating the robustness of an extension to redox chemistry modeling by means of a combination of DFT calculations with the experimental results. In agreement with the experimental evidence from cyclic voltammetry, the initial one electron reduction of the $[Pt^{IV}(NH_3)_2(CH_3COO)_2Cl_2]$ complex occurs through a stepwise mechanism via a metastable hexacoordinated platinum(III) $[Pt^{III}(NH_3)_2(CH_3COO)_2Cl_2]^-$ intermediate and a subsequent acetate ligand detachment with an activation free energy of 0.28 eV (6.46 kcal mol^{-1}). On the other hand, the second electron reduction of the resulting pentacoordinated $[Pt^{III}(NH_3)_2(CH_3COO)Cl_2]$ species occurs through a barrierless concerted process to the final $[Pt^{II}(NH_3)_2(CH_3COO)_2]$ derivative.

Supporting Information Available:

Differences between PB and C-PCM solvation methods (Table S1), relative enthalpy and Gibbs free energy values at 298 K for the reaction profile (Tables S2-S5), natural bond orbital charges (Tables S6), natural bond orbital analysis of MP2/aug-cc-pVTZ results in the gas phase (Table S7), as well as graphical representations of the reaction profile for the two-electron reduction of the six-coordinated Pt(IV) complex in solution (Figures S1, S2).

References

(1) Rosenberg, B.; Van Camp, L.; Trosko, J. E.; Mansour, V. H. Platinum Compounds: a New Class of Potent Antitumour Agents. *Nature* **1969**, *222*, 385–387.

(2) Sherman, S. E.; Lippard, S. J. Structural Aspects of Platinum Anticancer Drug Interactions with DNA. *Chem. Rev.* **1987**, *87*, 1153–1181.

(3) Reedijk, J. Improved Understanding in Platinium Antitumour Chemistry. *Chem. Commun.* **1996**, *7*, 801–806.

(4) Jamieson, E. R.; Lippard, S. J. Structure, Recognition, and Processing of Cisplatin-DNA Adducts. *Chem. Rev.* **1999**, *99*, 2467–2498.

(5) Wong, E.; Giandomenico, C. M. Current Status of Platinum-Based Antitumor Drugs. *Chem. Rev.* **1999**, *99*, 2451–2466.

(6) Wang, D.; Lippard S. J. Cellular Processing of Platinum Anticancer Drugs. *Nat. Rev. Drug Discov.* **2005**, *4*, 307–320.

(7) Jung, Y.; Lippard, S. J. Direct Cellular Responses to Platinum-Induced DNA Damage. *Chem. Rev.* **2007**, *107*, 1387–1407.

(8) Arnesano, F.; Natile, G. Mechanistic Insight into the Cellular Uptake and Processing of Cisplatin 30 Years after its Approval by FDA. *Coord. Chem. Rev.* **2009**, *253*, 2070–2081.

(9) Klein, A. V.; Hambley, T. W. Platinum Drug Distribution in Cancer Cells and Tumors. *Chem. Rev.* 2009, *109*, 4911–4920.

(10) Harrison, R. C.; McAuliffe, C. A.; Zaki, A. M. An Efficient Route for the Preparation of Highly Soluble Platinum (II) Antitumour Agents. *Inorg. Chim. Acta* **1980**, *46*, L15–L16.

(11) Harrap, K. R. Preclinical Studies Identifying Carboplatin as a Viable Cisplatin Alternative. *Cancer Treat. Rev.* **1985**, *12*, 21–33.

(12) Boulikas, T.; Vougiouka, M. Cisplatin and Platinum Drugs at the Molecular Level. *Oncol. Rep.* **2003**, *10*, 1663–1682.

(13) Davies, M. S.; Fenton, R. R.; Huq, F.; Ling, E. C.; Hambley, T. W. Studies on the Nature and Strength of Pt... H (-N) Interactions. The Crystal Structures of Chloro [N-(2-aminoethyl)-N-(2-ammonioethyl)ethane-1,2-diamine] Platinum (II) Chloride and Dichloro [4,7-diaza-1-azoniacyclononane] Platinum (II) Tetrachlor. *Aust. J. Chem.* **2000**, *53*, 451–456.

(14) Ali, M. S.; Powers, C. A.; Whitmire, K. H.; Guzman-Jimenez, I.; Khokhar, A. R. Synthesis, Characterization, and Representative Crystal Structure of Lipophilic Platinum II (Homopiperazine) Carboxylate Complexes. *J. Coord. Chem.* **2001**, *52*, 273–287.

(15) Mukhopadhyay, U.; Thurston, J. H.; Whitmire, K. H.; Khokhar, A. R. Synthesis and Characterization of *Cis*-bis-heptamethyleneimine Platinum (II) Dicarboxylate Complexes: Crystal Structure of *Cis*-[Pt(heptamethyleneimine)$_2$malonate)]·H_2O. *Polyhedron* **2002**, *21*, 2369–2374.

(16) Luzyanin, K. V.; Gushchin, P. V.; Pombeiro, A. J.; Haukka, M.; Ovcharenko, V. I.; Kukushkin, V. Y. Oxidation of Pt-bound Bis-hydroxylamine as a Novel Route to Unexplored Dinitrosoalkane Ligated Species. *Inorg. Chem.* **2008**, *47*, 6919-6930.

(17) Wexselblatt, E.; Gibson, D. What Do We Know about the Reduction of Pt (IV) Pro-Drugs? *J. Inorg. Biochem.* **2012**, *117*, 220–229.

(18) Platts, J. A.; Ermondi, G.; Caron, G.; Ravera, M.; Gabano, E.; Gaviglio, L.: Pelosi, G.; Osella, D. Molecular and Statistical Modeling of Reduction Peak Potential and Lipophilicity of Platinum (IV) Complexes. *J. Biol. Inorg. Chem.* **2011**, *16*, 361–372.

(19) McCormick, M. C.; Keijzer, K.; Polavarapu, A.; Schultz, F. A.; Baik, M. H. Understanding Intrinsically Irreversible, Non-Nernstian, Two-Electron Redox Processes: A Combined Experimental and Computational Study of the Electrochemical Activation of Platinum (IV) Antitumor Prodrugs. *J. Am. Chem. Soc.* **2014**, *136*, 8992–9000.

(20) Bochevarov, A. D.; Harder, E.; Hughes, T. F.; Greenwood, J. R.; Braden, D. A.; Philipp, D. M.; Rinaldo, D.; Halls, M. D.; Zhang, J.; Friesner, R. A. Jaguar: A High-Performance Quantum Chemistry Software Program with Strengths in Life and Materials Sciences. *Int. J. Quantum Chem.* **2013**, *113*, 2110–2142.

(21) Jaguar version 7.5, Schrodinger LLC, New York NY, **2008**.

(22) Gaussian 09, Revision A.02, Gaussian, Inc., Wallingford CT, **2016**.

(23) Becke, A. D. Becke's Three Parameter Hybrid Method Using the LYP Correlation Functional. *J. Chem. Phys.* **1993**, *98*, 5648–5652.

(24) Stephens, P. J.; Devlin, F. J.; Chabalowski, C.; Frisch, M. J. Ab Initio Calculation of Vibrational Absorption and Circular Dichroism Spectra Using Density Functional Force Fields. *J. Phys. Chem.* **1994**, *98*, 11623–11627.

(25) Niu, S.; Hall, B. M. Theoretical Studies on Reactions of Transition-Metal Complexes. *Chem. Rev.* **2000**, *100*, 353–405.

(26) Nielsen, R. J.; Keith, J. M.; Stoltz, B. M.; Goddard, W. A. III. A Computational Model Relating Structure and Reactivity in Enantioselective Oxidations of Secondary Alcohols by (−)-Sparteine−Pd^{II} Complexes. *J. Am. Chem. Soc.* **2004**, *126*, 7967–7974.

(27) Battle, A. R.; Platts, J. A.; Hambley, T. W.; Deacon, G. B. Synthesis, Spectroscopy, and Theoretical Studies of Platinum (II) Phosphate Complexes. *J. Chem. Soc., Dalton Trans.* **2002**, *9*, 1898–1902.

(28) Burda, J. V.; Leszczynski, J. How Strong can the Bend be on a DNA Helix from Cisplatin? DFT and MP2 Quantum Chemical Calculations of Cisplatin-Bridged DNA Purine Bases. *Inorg. Chem.* **2003**, *42*, 7162–7172.

(29) Pavelka, M.; Lucas, M. F. A.; Russo, N. On the Hydrolysis Mechanism of the Second-Generation Anticancer Drug Carboplatin. *Chem. Eur. J.* **2007**, *13*, 10108–10116.

(30) Ciancetta, A.; Coletti, C.; Marrone, A.; Re, N. Activation of Carboplatin by Chloride Ions: a Theoretical Investigation. *Theor. Chem. Acc.* **2011**, *129*, 757–769.

(31) Ciancetta, A.; Coletti, C.; Marrone, A.; Re, N. Activation of Carboplatin by Carbonate: a Theoretical Investigation. *Dalton Trans.* **2012**, *41*, 12960–12969.

(32) Graziani, V.; Coletti, C.; Marrone, A.; Re, N. Activation and Reactivity of a Bispidine Analogue of Cisplatin: A Theoretical Investigation. *J. Phys. Chem. A* **2016**, *120*, 5175–5186.

(33) Šebesta, F.; Burda, J. V. Side Reactions with an Equilibrium Constraint: Detailed Mechanism of the Substitution Reaction of Tetraplatin with dGMP as a Starting Step of the Platinum (IV) Reduction Process. *J. Phys. Chem. B* **2017**, *121*, 4400–4413.

(34) Ritacco, I.; Mazzone, G.; Russo, N.; Sicilia, E. Investigation of the Inertness to Hydrolysis of Platinum (IV) Prodrugs. *Inorg. Chem.* **2016**, *55*, 1580–1586.

(35) Zhao, Y.; Truhlar, D. G. The M06 Suite of Density Functionals for Main Group Thermochemistry, Thermochemical Kinetics, Noncovalent Interactions, Excited States, and Transition Elements: Two New Functionals and Systematic Testing of Four M06-Class Functionals and 12 Other Functionals. *Theor. Chem. Acc.* **2008**, *120*, 215–241.

(36) Yanai, T.; Tew, D.; Handy, N. A New Hybrid Exchange-Correlation Functional Using the Coulomb-Attenuating Method (CAM-B3LYP). *Chem. Phys. Lett.* **2004**, *393*, 51–57.

(37) Grimme, S.; Antony, J.; Ehrlich, S.; Krieg S. A Consistent and Accurate Ab Initio Parametrization of Density Functional Dispersion Correction (DFT-D) for the 94 Elements H-Pu. *J. Chem. Phys.* **2010**, *132*, 154104.

(38) Frisch, M. J.; Head-Gordon, M..; Pople, J. A. Direct MP2 Gradient Method. *Chem. Phys. Lett*. **1990**, *166*, 275–280.

(39) Frisch, M. J.; Head-Gordon, M.; Pople, J. A. Semi-Direct Algorithms for the MP2 Energy and Gradient. *Chem. Phys. Lett.* **1990**, *166*, 281–289.

(40) Head-Gordon, M.; Pople, J. A.; Frisch, M. J. MP2 Energy Evaluation by Direct Methods. *Chem. Phys. Lett.* **1988**, *153*, 503–506.

(41) De Petris, A.; Ciavardini, A.; Coletti, C.; Re, N.; Chiavarino, B.; Crestoni, M. E.; Fornarini, S. Vibrational Signatures of the Naked Aqua Complexes from Platinum (II) Anticancer Drugs. *J. Phys. Chem. Lett.* **2013**, *4*, 3631 – 3635.

(42) Hay, P. J.; Wadt, W. R. Ab Initio Effective Core Potentials for Molecular Calculations. Potentials for K to Au Including the Outermost Core Orbitals. *J. Chem. Phys.* **1985**, *82*, 299–310.

(43) Dunning Jr, T. H. Gaussian Basis Sets for Use in Correlated Molecular Calculations. I. The Atoms Boron through Neon and Hydrogen. *J. Chem. Phys.* **1989**, *90*, 1007–1023.

(44) Kendall, R. A.; Dunning Jr, T. H.; Harrison, R. J. Electron Affinities of the First-Row Atoms Revisited. Systematic Basis Sets and Wave Functions. *J. Chem. Phys.* **1992**, *96*, 6796–6806.

(45) Woon, D. E.; Dunning Jr, T. H. Gaussian Basis Sets for Use in Correlated Molecular Calculations. III. The Atoms Aluminum through Argon. *J. Chem. Phys.* **1993**, *98*, 1358–1371.

(46) Tannor, D. J.; Marten, B.; Murphy, R.; Friesner, R. A.; Sitkoff, D.; Nicholls, A.; Ringnalda, M.; Goddard, W. A. III; Honig, B. Accurate First Principles Calculation of Molecular Charge Distributions and Solvation Energies from Ab Initio Quantum Mechanics and Continuum Dielectric Theory. *J. Am. Chem. Soc.* **1994**, *116*, 11875–11882.

(47) Corinti, D.; Coletti, C.; Re, N.; Chiavarino, B.; Crestoni, M. E.; Fornarini, S. Cisplatin Binding to Biological Ligands Revealed at the Encounter Complex Level by IR Action Spectroscopy. *Chem. Eur. J.* **2016**, *22*, 3794–3803.

(48) Corinti, D.; Coletti, C.; Re, N.; Piccirillo, S.; Giampà, M.; Crestoni, M. E.; Fornarini, S. Hydrolysis of Cis- and Transplatin: Structure and Reactivity of the Aqua Complexes in a Solvent Free Environment. *RSC Adv.* **2017**, *26*, 15877–15884.

(49) Paciotti, R.; Corinti, D.; De Petris, A.; Ciavardini, A.; Piccirillo, S.; Coletti, C.; Re, N.; Maitre, P.; Bellina, B.; Barran, P.; Chiavarino, B. Cisplatin and Transplatin Interaction with Methionine: Bonding Motifs Assayed by Vibrational Spectroscopy in the Isolated Ionic Complexes. *Phys. Chem. Chem. Phys.* **2017,** *19*, 26697–26707.

(50) Baik, M. H.; Friesner, R. A. Computing Redox Potentials in Solution: Density Functional Theory as a Tool for Rational Design of Redox Agents. *J. Phys. Chem. A* **2002**, *106*, 7407–7412.

(51) Coskun, D.; Jerome, S. V.; Friesner, R. A. Evaluation of the Performance of the B3LYP, PBE0, and M06 DFT Functionals, and DBLOC-Corrected Versions, in the Calculation of Redox Potentials and Spin Splittings for Transition Metal Containing Systems. J. Chem. Theory Comput. **2016**, *12*, 1121–1128.

(52) Broere, D. L.; De Bruin, B.; Reek, J. N.; Lutz, M.; Dechert, S.; Van Der Vlugt, J. I. Intramolecular Redox-Active Ligand-to-Substrate Single-Electron Transfer: Radical Reactivity with a Palladium (II) Complex. *J. Am. Chem. Soc.* **2014**, *136*, 11574–11577.

(53) Shopov, D. Y.; Rudshteyn, B.; Campos, J.; Batista, V. S.; Crabtree, R. H.; Brudvig, G. W. Stable Iridium (IV) Complexes of an Oxidation-Resistant Pyridine-Alkoxide Ligand: Highly Divergent Redox Properties Depending on the Isomeric Form Adopted. *J. Am. Chem. Soc.* **2015**, *137*, 7243–7250.

(54) Demissie, T. B.; Ruud, K.; Hansen, J. H. DFT as a Powerful Predictive Tool in Photoredox Catalysis: Redox Potentials and Mechanistic Analysis. *Organometallics* **2015**, *34*, 4218–4228.

For Table of Contents Only

The accurate DFT and MP2 calculations allowed us to formulate the detailed mechanism for the two-electron reduction of the $[Pt^{IV}(NH_3)_2(CH_3COO)_2Cl_2]$ complex. The initial one electron reduction of the Pt^{IV} complex occurs through a stepwise mechanism via a metastable hexacoordinated Pt^{III}–intermediate and a subsequent acetate ligand detachment with an activation free energy of 5.1 kcal mol^{-1}. The second electron reduction of the resulting pentacoordinated Pt^{III} species occurs through a barrierless concerted process.

Table of Contents Graphic (For Table of Contents Only)